

Recent Developments in Microwave Ion Clocks

John D. Prestage, Robert L. Tjoelker and Lute Maleki

*California Institute of Technology, Jet Propulsion Laboratory
4800 Oak Grove Drive
Building 298
Pasadena, CA 91104*

Abstract. In this paper we review the development of microwave frequency standards based on trapped ions. Following two distinct paths, microwave ion clocks have evolved greatly in the last twenty years since the earliest Paul trap-based units. Laser cooled ion frequency standards reduce the second order Doppler shift from ion micro-motion and thermal secular motion achieving good signal-to-noise via cycling transitions where as many as $\sim 10^8$ photons per second per ion may be scattered. Today, laser-cooled ion standards are based on linear Paul traps which hold ions near the node line of the trapping electric field minimizing micro-motion at the trapping field frequency and the consequent 2nd order Doppler frequency shift. These quadrupole (radial) field traps tightly confine tens of ions to a crystalline single line structure. As more ions are trapped, space charge forces some ions away from the node-line axis and the 2nd Doppler grows larger, even at negligibly small secular temperatures. Buffer gas cooled clocks rely on large numbers of ions, typically $\sim 10^7$, optically pumped by a discharge lamp at a scattering rate of a few photons per second per ion. To reduce the 2nd Doppler shift from space charge repulsion of ions from the trap node line, novel multi-pole ion traps are now being developed where ions are weakly bound with confining fields that are effectively zero through the trap interior and grow rapidly near the trap electrode ‘walls.’

INTRODUCTION

Microwave ion frequency standards are promising candidates for both ultra-stable and ultra-accurate clock applications. The atomic clock with the best short-term stability yet demonstrated is based on buffer-gas cooled, discharge lamp pumped $^{199}\text{Hg}^+$ ions confined in a linear trap [1]. Similarly, a laser-cooled linear crystal of tens of $^{199}\text{Hg}^+$ confined in a linear trap is expected to show clock accuracy approaching 10^{-16} , exceeding the accuracy of the best present day cesium fountain clocks [2]. The development of these ion clocks has followed very different design pathways carried out to meet very different goals. For example, ensembles of continuously- operating high-stability clocks are used in time scales throughout the world and must be reliable. Similarly, deep space navigation via Doppler spacecraft tracking and ranging and VLBI radio astronomy both rely on ultra-stable, continuously operating microwave standards. Earth orbiting GPS/Navstar satellites enable precise navigation anywhere on Earth and are based on small, low-power atomic clocks. By comparison, primary standards strive for absolute accuracy, above all other considerations, and whether based on trapped ions or neutral cesium, they are usually not continuously operating, portable, etc. There are many excellent reviews of ion trapping and ion clocks surveying laboratory standards where continuous operation has not been a goal [3-6]. This review will focus on high-stability, continuously operating ion clocks where simplicity in the full clock package has driven many of the design decisions.

There are many fundamental reasons why trapped ion microwave standards make excellent clocks. Since there are no wall collisions to re-populate a state prepared two level ion (T_1 relaxation) or to destroy atomic coherence (T_2 relaxation), very high resolution can be achieved in observing the clock transition. Typical room temperature $^{199}\text{Hg}^+$ buffer gas cooled clocks have demonstrated linewidths as narrow as 30 mHz on the 40 GHz clock transition, corresponding to an atomic line-Q of over 10^{12} [7]. Laser cooled beryllium ions [8] and mercury [2] ions have both shown T_1 and T_2 relaxation times longer than 100 s. Because T_1 is so long for trapped ions, optical pumping into one of the ground state hyperfine levels can be accomplished with a

discharge lamp and light scattering rates of only a few photons per second per atom. This has been done in the case of trapped $^{199}\text{Hg}^+$ ions with a ^{202}Hg lamp. Isotope shift and lack of hyperfine structure in a ^{202}Hg lamp spectrum can be used to excite the $\sim 194 \text{ nm } S_{1/2}(F=1)\delta P_{1/2}(F=1,2) \text{ } ^{199}\text{Hg}^+$ transition without exciting the $S_{1/2}(F=0)\delta P_{1/2}(F=1,2)$. In 1 to 2 seconds, most ions are pumped into the $S_{1/2}(F=0)$ clock level. Similar isotopic pumping might be possible in trapped $^{111,113}\text{Cd}^+$ ions with a ^{110}Cd lamp since the spectral overlap is similar to that in Hg ion isotopes [9].

In reviewing and comparing the various microwave ion-clock technologies there are a few general principles to keep in mind. The short-term stability $\sigma_y(\tau)$ is determined by the frequency of the atomic clock transition f_0 its frequency width Δf and the signal-to-noise SNR in the measured transition. This signal-to-noise is determined by the signal size measured at the half maximum point, S_{half} and the shot noise in the number of detected fluorescent uv/optical photons $\sqrt{S_{half} + B}$ where B is the amount of background collected light not contributing to the signal giving $SNR = S_{half} / \sqrt{S_{half} + B}$. The fractional measure of clock stability is

related to these clock parameters by $\sigma_y(\tau) = \frac{\Delta f}{\pi f_0 SNR} \sqrt{\frac{T_c}{\tau}}$ where T_c is the time required for a single

measurement cycle. The cycle time, T_c is the microwave resonance time T_R plus a ‘dead time’ T_D during which optical pumping, etc. are carried out. The resonance time T_R determines the linewidth ($\Delta f = 1/2T_R$ for a Ramsey pulse and $\Delta f \cong 0.8/T_R$ for a Rabi pulse). Because the total measuring time τ is composed of a sequence of M discrete measurements of duration T_c , $\tau/T_c = M$ and $\sigma_y(\tau)$ thus diminishes as $M^{-1/2}$, as in any measurement carried out identically M independent times. All microwave ion clocks follow a $\tau^{-1/2}$ behavior over some span of time but no clock can follow this improvement over indefinitely long averaging times because the measurements cannot all be strictly identical.

Since all ion microwave standards rely on state selection via optical pumping for atomic state interrogation, this expression is valid when the number of *detected* fluorescent photons is less than of order one per ion. This condition is certainly true for lamp excited systems where only a few photons per second are scattered per ion and those photons are detected with efficiencies that can approach 3-4% at best. But laser based ion standards can scatter many photons per second per ion and even *detect* several photons per ion per measurement cycle.

During clock operation, measurements are made alternately on either side of microwave atomic line center at half maximum of the transition probability. Following the microwave interrogation the ion is left in a coherent superposition of the upper and lower clock states. Optical state interrogation will then ‘project’ the ion into one of the two clock states with $\sim 50\%$ probability for finding the ion in each state. The quantum projection noise associated with the measurement process will then dominate over the photon counting shot noise described earlier if several photons are detected per ion. The clock noise then follows

$\sigma_y(\tau) = \frac{\Delta f}{\pi f_0 \sqrt{N}} \sqrt{\frac{T_R}{\tau}}$ where N is the number of trapped ions. We have assumed the resonance

interrogation time $T_R = \frac{1}{2\Delta f}$ (Ramsey pulse) is much longer than the dead time, T_D , so that $T_c \approx T_R$.

This relatively slow $\tau^{-1/2}$ improvement in resolution can lead to some constraints in the practice of clock development and testing. For example, to test a clock with accuracy 10^{-16} , the short-term noise should be significantly better than $10^{-13}/\tau^{1/2}/\text{Hz}^{1/2}$ since otherwise, 10^6 s ($>11 \text{ d}$) would be required to reduce the statistical noise to the 10^{-16} level.

The validity of the above short-term noise expressions also assumes that the stability of the interrogating local oscillator (LO) is much better than the single measurement stability level of the microwave atomic clock. This is seldom true with today’s trapped ion frequency standards, which operate with high SNR and high line $Q(=f_0/\Delta f)$. Because the cycle time T_c is more than the actual interrogation time where the LO frequency is

compared to the atomic coherence, the LO is unmonitored briefly during each measurement. This time period is required for ion state selection/optical pumping. The LO can then execute a random walk in phase, equivalent to a white frequency noise which degrades the performance from that given by the above clock noise estimate. Much analysis of this LO degradation of the performance has been done over the past several years [10,11].

Another consideration regarding microwave frequency standards based on hyperfine clock transitions is the inherent sensitivity to changes in the ambient magnetic field H_0 at the atom or ion. All such standards are based on transitions that show a quadratic magnetic-field dependence of the transition frequency $\nu = \nu_0 + C_H H_0^2$ where $C_H \propto 1/\nu_0$. Consequently, the fractional frequency sensitivity to changes in the magnetic field, $\frac{1}{\nu_0} \frac{\partial \nu}{\partial H_0} \propto \frac{H_0}{\nu_0^2}$. Thus, to minimize this source of frequency instability, a clock should be operated at low field H_0 , and have a large zero field hyperfine splitting, ν_0 . All accurate primary standards rely on occasional measurement of a linear Zeeman atomic transition to calibrate this frequency offset. Nevertheless, time variation of H_0 between linear Zeeman measurements will degrade clock stability according to the above scaling.

Until 1989 trapped ion microwave clocks were based on a conventional Paul rf trap where ions are trapped around a nodal point of the rf electric field at the center of symmetry of a three electrode geometry [4]. The 3 electrodes are each hyperbolic in shape and create a spherically harmonic pseudo-potential well when combinations of dc and ac fields are applied [4]. The confinement of a single laser-cooled ion in this trap can show quantum properties of an ion in the lowest quantum state of the potential well of the trap. A microwave clock based on this single ion would have a very small second order Doppler shift of the clock transition frequency but quantum projection noise would degrade the stability to the extent that operation as a clock would not be useful. As more ions are added to improve its stability, ion-ion repulsion would hold ions away from the node of the trap consequently inducing micro-motion and even chaotic rf-heating [12,13] of the ions, increasing the second-order Doppler frequency pulling. This sacrifice of clock accuracy for the sake of improving short-term stability can be circumvented by use of a linear ion trap [14]. The linear trap replaces the point node by a line of nodes and permits many laser-cooled ions to be trapped with micro-motion as small as a single ion in a conventional Paul trap.

LASER-COOLED STANDARDS

Most microwave laboratory ion standards are based on laser cooled ions in a linear Paul trap. Recent work has focused primarily on $^{199}\text{Hg}^+$ [2] and $^{171}\text{Yb}^+$ [15], with some work on $^{111,113}\text{Cd}^+$ [9] in a conventional Paul trap. There has also been work on laser cooled $^9\text{Be}^+$ ion clouds in a Penning trap where ion confinement is accomplished with static magnetic and electric fields [8]. The relevant energy levels for these ions are shown in Figure 1 along with the optical pumping transitions.

A laser cooled $^{199}\text{Hg}^+$ clock under development [2] is very promising as a primary standard with accuracy approaching the 10^{-16} level, which would surpass the accuracy of present day neutral ^{133}Cs fountain clocks by an order of magnitude. This clock is based on a small linear trap (~ 2 mm diameter by ~ 4 mm long) where a laser cooled crystalline ‘string’ of 7 ions are interrogated at 40.5 GHz using the Ramsey technique. Because the vacuum walls are liquid-He cooled to 4K, there are very few background gas molecules to collisionally heat

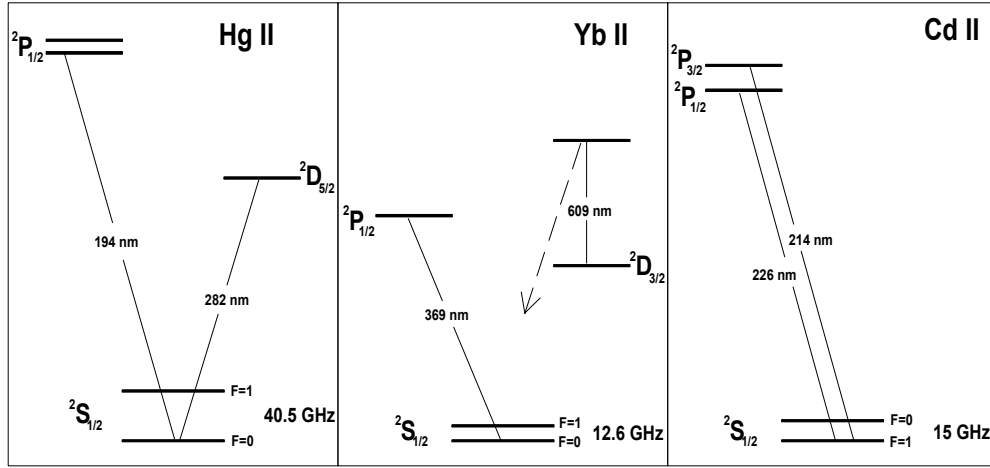


Figure 1. Energy levels for $^{199}\text{Hg}^+$, $^{171}\text{Yb}^+$, and $^{113,111}\text{Cd}^+$ for use as microwave frequency standards.

the ions when the cooling laser is shut off for the 100 s microwave interrogation. Separate measurements show that the ion secular temperature remains under 25 mK during the 100 s ‘laser-off’ period.

The trap operates in a static magnetic field of 3 mG. The largest known uncalibrated frequency offset stems from a quadratic Zeeman shift of the clock transition from (asymmetric) ac currents flowing in the trap rods at the trap drive frequency to generate the ac trapping electric field in a trap with unbalanced trap rod capacitances. This leads to a frequency shift of the clock transition linear in the trap drive power dissipation, and under typical clock operation is about $5(3.2) \times 10^{-15}$. The short-term frequency stability of the standard with 7 ions and $T_R=100$ s was measured to be $3.3 \times 10^{-13} \text{ (TM)}^{-1/2} \text{ Hz}^{-1/2}$. During the optical pumping process, about 150 photons were detected per ion during each measurement cycle. The excess above the quantum projection noise under these conditions, $1.5 \times 10^{-13} \text{ (TM)}^{-1/2} \text{ Hz}^{-1/2}$, is due to 194 nm laser intensity and frequency fluctuations from measurement to measurement. Improvements in accuracy to the 10^{-16} level will follow the development of a smaller trap requiring lower voltage and operated at a lower frequency so that the ac Zeeman shift from any asymmetric currents in the trap rods is substantially smaller. Additionally, more ions can be trapped and individually monitored to reach the projection noise limit.

A laser cooled $^{171}\text{Yb}^+$ microwave ion standard is under development [15] where $\sim 10^4$ ions are cooled to below 1 K in a linear trap (~ 20 mm diameter by ~ 60 mm length). The short-term stability is estimated from signal-to-noise, line-Q, and total measurement cycle time to be $5 \times 10^{-14} \text{ (TM)}^{1/2} / \text{Hz}^{1/2}$. This experiment has no cryo-cooling of the vacuum walls, and so, when the cooling laser is switched off for 12.6 GHz microwave interrogation, the ion heating rate is somewhat faster than the Hg^+ work at NIST. Measurements show that after 10 s the temperature has risen to ~ 1 K and after 20 s to ~ 3 K. Cooling and optical pumping are carried out with a 369 nm laser as shown in the Yb^+ energy level diagram of Fig 1. The presence of the metastable $^2\text{D}_{3/2}$ ($F=1$) state, into which ions can decay during the $^2\text{S}_{1/2}$ ($F=1$) δ $^2\text{P}_{1/2}$ ($F=0$) cycling transition and thus be removed from the cooling cycle, forces the use of a clearing laser at 609 nm. The largest sources of error in the accuracy assessment of this clock are 2^{nd} -order Doppler and 2^{nd} -order Zeeman, each estimated to be 2×10^{-15} .

LAMP-BASED STANDARDS

Because ions in a trap undergo very weak hyperfine population relaxation rates, ^{202}Hg rf discharge lamps can substantially optically pump $^{199}\text{Hg}^+$ ions into the $F=0$ ground state hyperfine level in one or two seconds. Pumping into this state proceeds with the scattering of only a few uv photons per ion and thus, a high signal-to-noise ratio in the measured clock resonance can only be achieved with large ion clouds, typically with 10^6

to 10^7 ions. Motivated by these constraints, we first recognized and developed the linear ion trap [14] for storage of ion clouds that were ten or more times larger than could be stored in a conventional Paul trap. As described earlier, the linear trap replaces the point node of the Paul trap with a line of nodes. Many times the number of ions can be trapped with the same mean distance to the node line of the electric field as compared to a conventional Paul trap. This is exactly analogous to the small laser-cooled ion clouds and linear crystals described above.

RECENT RESULTS WITH LITS/CSO COMBINATION

The original ^{199}Hg Linear Ion Trap Standard (LITS) developed at the JPL Frequency Standards Lab is typically operated with $\sim 10^7$ ions in a quadrupole linear trap of 25 mm diameter by 75 mm in length. Because the Hg^+ trapping time is finite and the clock is designed for continuous operation, ions are loaded for about 1 s per measurement cycle via an electron pulse through the trap center. A mercuric oxide (HgO) powder is heated to ~ 200 C producing a 10^{-10} Torr ambient vapor throughout the vacuum system. This background vapor limits the usable coherence time of the 40.5 GHz clock transition to about 10 s via charge exchange of a (coherent) state prepared ion with the parent neutral vapor. The trap time for the Hg^+ charge cloud is a few hours even though every 10 s or so each ion is replaced with another Hg ion in a random hyperfine state.

The LITS has shown excellent signal-to-noise in the measured clock transition as determined by the size of the ion resonance line and the level of stray light output from the ^{202}Hg lamp. Signal levels as high as 80,000 counts with a background of about 180,000 counts have been measured in a 1.5 s collection interval with dual fluorescence collection optical modules. These signal levels were measured with an 8 s Ramsey interrogation of the 40.5 GHz Hg^+ clock transition and yield a short-term clock performance $\sigma_y(\tau) = 2 \times 10^{-14}/\sqrt{\tau}/\oplus\text{Hz}$ as calculated from signal-to-noise and line Q. This short term performance exceeds the noise level for all other clocks except the very best cryogenic cavity microwave oscillators.

Recently, a cryogenic compensated sapphire oscillator (CSO) [1] has been developed in our lab and has been used to measure the un-degraded LITS performance. This continuously operating cryo-cooled liquid helium refrigerated sapphire cavity oscillator delivers short-term stability of a few parts in 10^{15} to a few hundred seconds and is adequate to measure the ion standard short-term performance. During this measurement the LITS calculated stability from signal-to-noise and line-Q was approximately $3 \times 10^{-14}/\sqrt{\tau}/\oplus\text{Hz}$ as was measured [1]. This shows that for short-term performance there are no additional noise sources larger than shot noise in the total collected uv light.

This measurement was carried out with a large ion cloud with a second-order Doppler shift of over 10^{-12} , with a potential for noise sources from Doppler instabilities. For this reason we have developed an extended linear ion trap [16] to exploit the mobility of charged ions that can be electrically transported from one end of a linear trap to another. This layout partitions a long linear trap into an optical interrogation region and an extension to carry out the microwave clock transition. The ions are moved from one region into another via a ~ 5 V dc voltage bias applied to the trapping rods of the region from which they are to be excluded. There are several advantages to this LITE architecture over the conventional arrangement, the primary advantage being that we can investigate the use of novel linear traps for ion storage during the microwave clock resonance interrogation. Optical pumping and state interrogation will be done in a conventional ‘optically open’ quadrupole linear trap that will permit fluorescence detection. The resonance trap has been designed to allow the ion cloud second order Doppler shift to be drastically reduced as described later in this article. Traps that are to be used for the microwave region are not required to be open for fluorescence light collection though they must allow microwaves to enter from outside.

HARMONIC LINEAR ION TRAPS

The harmonicity of a traditional four-rod linear ion trap is a function of rod diameter and spacing. Improved harmonicity can be accomplished with variations to this geometry. For example, Fig. 2 shows a linear ion trap

configuration based on a cylinder that has been cut along its length into eight sectors, four at 60° angular width and four at 30° angular width. The quadrupole symmetry requirement, $\Phi(\rho, \theta \pm \pi/2) = -\Phi(\rho, \theta)$, leads to the expansion for the potential inside any linear quadrupole trap

$$\Phi(\rho, \theta) = C_0 \rho^2 \sin(2\theta) + C_1 \rho^6 \sin(6\theta) + C_2 \rho^{10} \sin(10\theta) + \dots$$

If the 30° sectors are grounded and the remaining 60° sectors are biased in a quadrupole fashion as shown, the resulting field is very harmonic, i.e., $C_1 = 0$.

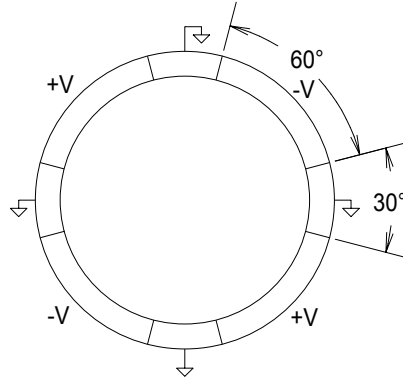


Figure 2. This linear quadrupole produces a very harmonic trap potential $\Phi(\rho, \theta) = C_0 \rho^2 \sin(2\theta) + C_2 \rho^{10} \sin(10\theta) + \dots$. The $C_1 \rho^6 \sin(6\theta)$ term is suppressed by the 30° grounded sections.

MULTI-POLE LINEAR ION TRAPS

Higher pole traps have been used as a tool in analytical chemistry to study ion-molecule low energy collisions and reactions [17]. Octopole rf electrodes act as a guide to transport ions from one location to another in similar applications. These applications involve very low densities of ions where space charge interactions within the ion cloud are inconsequential. Ions are detected directly with a channeltron electron multiplier. Because ions in a multi-pole rf trap spend relatively little time in the region of high rf electric fields there is very little rf heating and low temperature collisions can be studied.

The pseudo-potentials for quadrupolar trapping fields are equivalent to a uniform background pseudo-charge with a consequence that (cold) ion clouds fill the trap with uniform density. In lamp based clock applications, most of the second order Doppler shift for large ion clouds in a linear quadrupole trap is a consequence of the space charge Coulomb repulsion force that results from confining ions of like charge in a relatively small volume. These repulsive forces are balanced by the ponderomotive forces generated by ion motion in the rf electric field gradient. For large ion clouds, most of the motional energy is stored in the micro-motion necessary to generate the force to balance the space charge repulsion. For a typical cloud, buffer gas cooled to 500 K, the 2nd Doppler shift from rf micro-motion can be up to 3 times the secular motion contribution to the energy [18,19].

Since higher pole traps have not previously been used in clock applications, we shall review some properties of large ion clouds in multi-pole traps, where space-charge effects are non-negligible. The pseudo-potential, $V^*(r)$, for a particle of charge q and mass m , inside the linear multi-pole with $2k$ electrodes is given by [17]

$$V^*(r) = \frac{k^2}{16} \frac{q^2 U_0^2}{m \Omega^2 r_0^2} \hat{r}^{2k-2} \equiv \frac{k^2}{8} m \omega^2 r_0^2 \hat{r}^{2k-2}$$

The operating rf frequency is Ω radians per second, the trap inner radius is r_0 , and the amplitude of the rf voltage applied to each rod is $U_0/2$. (The peak voltage between neighboring trap electrodes is U_0). The normalized distance $\hat{r} = r/r_0$. The equation of motion for an ion in the time varying harmonic potential of a linear quadrupole is the Mathieu equation [3] and forms the basis for single amu mass selectivity in rf mass spectrometers, when combined with a static electric field. The electric field growth with radial distance from centerline is assumed to be linear with a constant growth in strength out to the trap electrodes. The Mathieu equation and its solutions determine those charge-to-mass's, q/m , whose trajectories are stable for the given trap dimensions, operating frequencies, applied voltages, etc. Unstable trajectories can result (in harmonic linear traps) when the extent of a particle's oscillatory micro-motion is comparable to its distance to the trap center. This can be reformulated as an adiabaticity requirement. Accordingly, for stable trapping, the change in the electric field amplitude over the extent of the particles oscillatory micro-motion must be less than the field amplitude [4].

In a higher pole trap, the rapid growth of the trapping fields near the electrodes can violate the adiabaticity requirement imposed on the motion of a charged particle to ensure stable trapping. By numerical computation of single particle trajectories [17] it is found that so long as the adiabaticity parameter

$$\eta = \frac{2q|\nabla E_0|}{m\Omega^2} = k(k-1) \frac{qU_0}{m\Omega^2 r_0^2} \hat{r}^{k-2} \leq 0.3 \equiv \eta_{\max}, \text{ then particles will be trapped in a stable orbit. In}$$

practice this means that for a particle to remain bound during its trajectory it cannot travel outside the radius

$$R_{\max} = r_0 \left[\frac{0.3}{k(k-1)} \frac{m\Omega^2 r_0^2}{qU_0} \right]^{\frac{1}{k-2}} \text{ where } k > 2. \text{ The well-depth in a multi-pole trap can be defined as the}$$

$$\text{value of the pseudo-potential at } R_{\max}, V^*(R_{\max}) = \frac{m\Omega^2 r_0^2}{16} \left[\frac{\eta_{\max}}{k-1} \right]^{2\frac{k-1}{k-2}} \left[\frac{1}{k} \frac{m\Omega^2 r_0^2}{qU_0} \right]^{\frac{2}{k-2}}. \text{ Unlike the}$$

quadrupole trap, the well depth diminishes as the trapping voltage U_0 increases. As k gets large $V^*(R_{\max})$

$$\text{approaches } V^*_{k \gg 1}(R_{\max}) = \frac{m\Omega^2 r_0^2}{k^2} \frac{\eta_{\max}^2}{16}, \text{ showing that the well depth decreases as the square of the}$$

number of multi-poles, but increases with particle mass, trap operating frequency and size. For higher pole traps the well depth becomes insensitive to the trap operating voltage. This is very different behavior from a

linear quadrupole trap where the transverse well-depth scales as $\frac{q^2 U_0^2}{m\Omega^2 r_0^2}$ [20].

To understand space-charge interactions, we have solved the Boltzman equation to find the thermal equilibrium density distribution of ions at temperature T held in the pseudo-potential well of the multi-pole trap. The radial density $n(r)$ of ions at temperature, T , held in the multipole trap is found from the Boltzmann distribution[18] $n(r) = n(0) \exp(-(V^*(r) + q\phi_{sc}(r))/k_B T)$ where $\phi_{sc}(r)$ and $n(r)$ are related through Poisson's equation $\nabla^2 \phi_{sc}(r) = -qn(r)/\epsilon_0$. This leads to the equation [19] for $n(r)$

$$n'' + \frac{n'}{r} - \frac{n'^2}{n} - \frac{n^2}{n_0 \lambda_D^2} = -k^2 (k-1)^2 \frac{n}{4\lambda_D^2} \hat{r}^{2k-4}$$

In this equation, $n_0 = 2\epsilon_0 m \omega^2 / q^2$ is the pseudo-charge density in quadrupole trap with secular frequency ω , produced by a quadrupole trap of the same operating parameters as the multi-pole and $\lambda_D^2 = k_B T / (2m\omega^2)$ is the Debye length for the ion plasma.

To compute the second-order Doppler shift for the ion cloud density distribution we must also know the

micro-motion velocity, v , throughout the ion trap. This is given by $\langle v^2 \rangle = \frac{k^2}{4} \omega^2 r_0^2 \hat{r}^{2k-2}$, where the

brackets $\langle \rangle$ indicate time averaging over a micro-motion cycle.

We solve the Boltzmann equation for the density profile by a fourth-order Runge-Kutta numerical technique. Typical operating conditions are 70 volts peak voltage between neighboring rods with a 1 MHz drive frequency. Assuming the Hg ions are at 300 K temperature we find a solution to the Boltzmann equation as shown in Figure 4 below. This density corresponds to 1.5×10^7 ions in a 25 cm long 12-pole trap. It is useful to define the normalized second order Doppler shift from the two dimensional micro-motion vs radial position as follows

$$\frac{-\left\langle \frac{v^2}{2c^2} \right\rangle}{-\frac{k_B T}{mc^2}} = \frac{k^2}{8} \frac{m \omega^2 r_0^2}{k_B T} \hat{r}^{2k-2} \equiv F_d^k(r)$$

Notice that the normalized 2nd order Doppler from the micro-motion is less than the ion thermal motion throughout most of the interior of the cloud.

Finally, we compute the total 2nd order Doppler from the micro-motion averaged across the ion cloud as

$$N_d^k = \frac{\int n(r) r F_d^k(r) dr}{\int n(r) r dr}.$$

From this calculation we find the total second order Doppler shift for the trapped ions with density profile $n(r)$

$$\frac{\Delta f}{f} = -\frac{3k_B T}{2mc^2} \left(1 + \frac{2}{3} N_d^k\right)$$

We can now evaluate this expression numerically for any multi-pole linear trap with a given total number of ions per unit length and temperature.

We first note that in the limit of small ion clouds where space charge effects are negligible, $\varphi_{sc} = 0$, and

N_d^k can be evaluated analytically giving $N_d^k = \frac{1}{k-1}$. Thus, in the linear quadrupole trap with only a small number of non-interacting ions, $N_d^{k=2} = 1$. This is a consequence of the equality of the average secular energy and average micro-motion energy in a harmonic (quadrupole) trap. As space charge interaction grows larger, $N_d = N_d^{k=2}$ increases. This number is as large as 3 for buffer gas cooled Hg ion clocks.

The 12-pole, by contrast, begins in the small cloud limit as $N_d^{k=6} = 1/5$, already 5 times smaller than the quadrupole. Additionally, because the field-free interior volume of the multi-pole is much larger than the quadrupole with the same radius, the low-density limit is satisfied with a much larger number of ions.

FIRST MULTI-POLE CLOCK OPERATION

We have built a 12-pole trap (Fig. 3) along with a co-linear quadrupole trap where ions are optically pumped between periods of microwave interrogation in the 12-pole. Ions have been successfully loaded into the quadrupole trap where the atomic fluorescence was measured with good signal to noise. The ions were then electrically shuttled into the co-linear 12-pole trap and then shuttled back into the quadrupole where fluorescence measurements show negligible ion loss in transport across the junction between the two traps. This also demonstrates that losses from the 12-pole trap were insignificant. This is important because the well depth of the 12-pole is around 0.3 eV as compared to the 3+ eV well depth of the linear quadrupole trap. The Boltzmann equation solutions outlined above can be used to investigate the ion cloud radial density profile in each of the two traps involved in this 12-pole Hg^+ ion clock. Ions are loaded into the quadrupole every cycle of the measurement simultaneous with the optical pumping of the ions that were just moved into the quadrupole from the 12-pole. For a typical operating condition $\sim 10^7$ ions are transferred back and forth in this manner. The

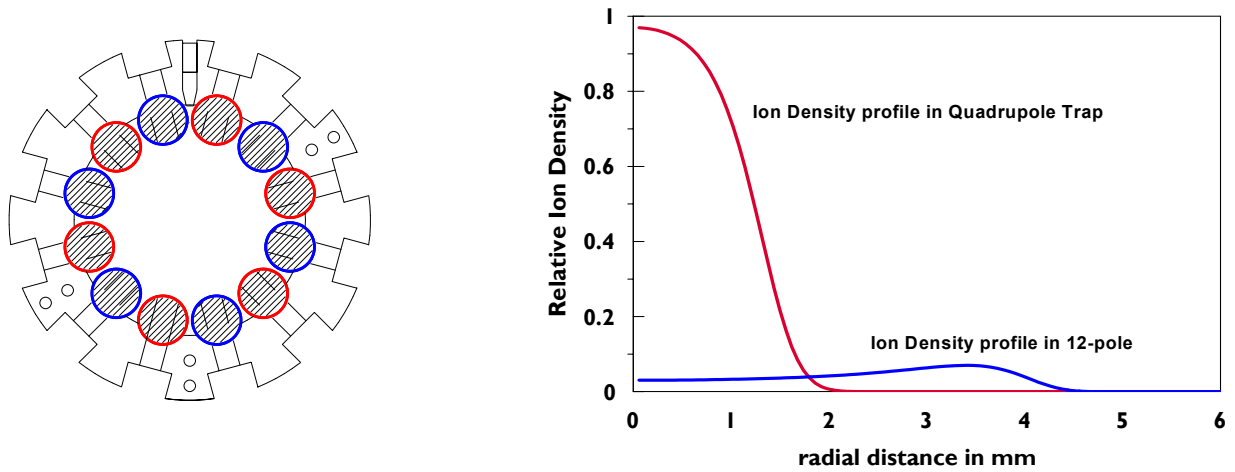


Figure 3. The linear 12-pole trap cross-section. The inner radius from center to first contact with the rod electrodes is 5.6 mm. Microwaves at frequency 40.5 GHz enter the trap between rods as shown at '12 o'clock' via a small (1x2mm) dielectric filled waveguide and horn.

Figure 4. The ion (radial) density distributions for $\sim 10^7$ ions in both the quadrupole (red) and in the 12-pole (blue). The 12-pole described here is ~ 3.8 times longer than the quadrupole further reducing the ion density inside the 12-pole. The central density falls by ~ 16 as ions are shuttled into the 12-pole resonance trap.

density inside the 12-pole is much weaker than inside the quadrupole, in part because the 12-pole trap is 3.8 times the length of the quadrupole. The bigger reduction in density comes from the nature of the multipole where the fields are very small until about 4.5 mm from center. The comparison of the two profiles is shown in Figure 4. The quadrupole is operated at $U_0 \sim 280$ V while the 12-pole is run at $U_0 \sim 30$ V with both at 1 MHz.

Conventional linear trap Hg standards developed in our lab show a $1-2 \times 10^{-12}$ frequency offset as the trap is loaded with ions in order to achieve a good signal-to-noise in the clock transition. The normalized micromotion 2nd order Doppler shift can be in effect much 'hotter' than the secular, that is, $N_d^{k=2}$ can be as large as 3. But there is some heating of the secular temperature when there is so much micromotion with a large cloud. We have measured the sensitivity of the Hg 40.5 GHz clock resonance frequency to changes in

ion number in the resonance trap. The 12-pole, with the greatly reduced micro-motion ($N_d^{k=6}=1/5$) is naturally much less sensitive to such space-charge and rf-heating problems. The measured frequency pulling of the clock transition as ion number is changed in both a quadrupole trap and in the 12-pole are shown together in Figure 5. In this data the number of trapped ions is controlled by the end-pin voltage, that is, as end-pin voltage is reduced below ~ 10 V fewer ions are trapped. This is a consequence of loading rates and loss rates in the vicinity of the electron gun where ions are created.

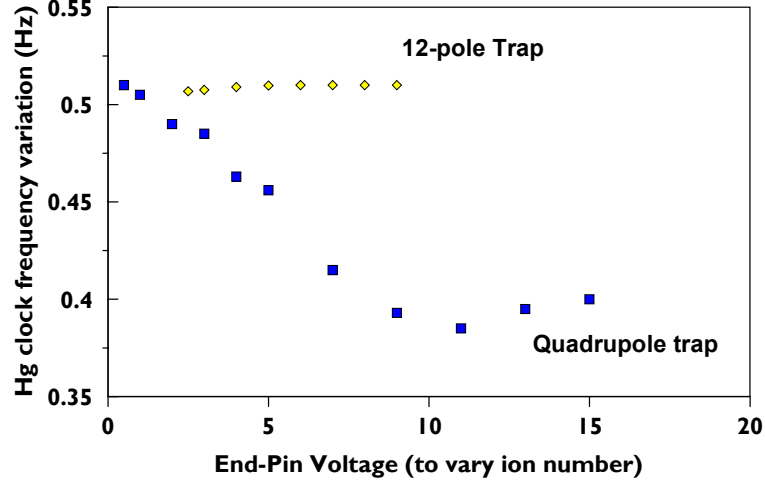


Figure 5. Variation of the Hg clock frequency with ion number. As the end-pin voltage diminishes to less than ~ 5 volts, fewer ions are held in these two linear traps. For the 12-pole trap, the half-signal point is 3-4 V while the quadrupole trap reaches half-signal as the end-pin voltage falls below 5-6 V. This is an artifact of the electron optics and loading rates for each trap. As can be seen, the 12-pole is drastically less sensitive than the quadrupole to variations in ion number for the same large cloud ($\sim 10^7$ ions) conditions. In both traps, the low end-pin voltage operation has less than $\sim 5\%$ of the total number of ions as the high voltage operation.

The clock operation of the 12-pole is carried out with a 6 second Rabi pulse applied to the ions after they have been optically pumped in the quadrupole trap and then transferred into the multi-pole trap. The signal size for the resonance is $\sim 50,000$ on the peak of the resonance curve with a background stray light level of $\sim 220,000$. The time required for a single measurement cycle is about 11 s. These parameters predict a short-term Allan deviation (limited by photon counting statistics) of $\sim 7 \times 10^{-14} / \sqrt{\text{Hz}} / \text{Hz}^{1/2}$. Figure 6 shows the LITE 12-pole clock stability measured against a hydrogen maser (SAO-26) demonstrating a slight degradation by the H-maser as an LO. This 7-day continuous measurement of the 12-pole stability was limited by the maser frequency instabilities beyond $\sim 30,000$ s averaging times. A second LITE 12-pole will soon be operational and will allow much lower noise floor measurements.

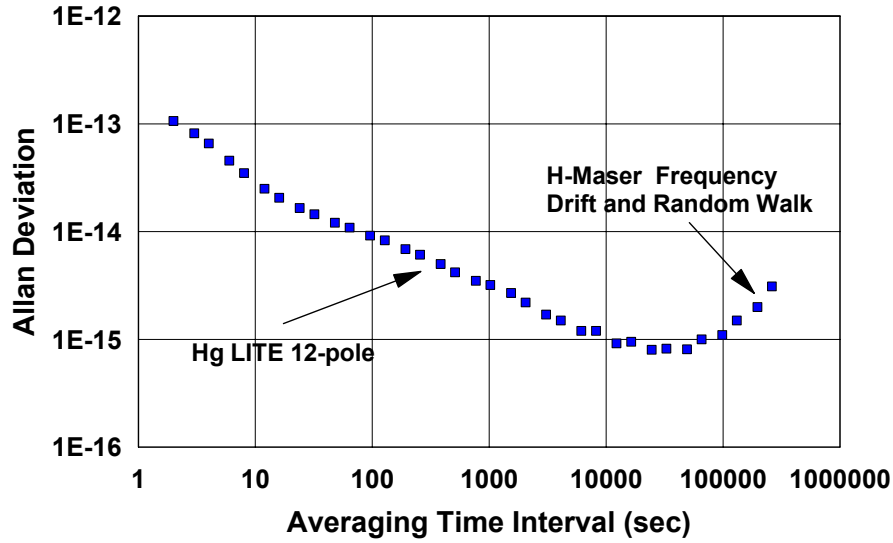


Figure 6. Measured Allan deviation for the LITE 12-pole Hg^+ ion clock vs a hydrogen maser.

The leading frequency offsets for the 12-pole configuration are listed in the table below. Changes in these offsets will lead to clock frequency instabilities. Accuracy approaching 10^{-14} may be practical in a rack mountable Hg clock based on the multi-pole linear trap. Use of the multi-pole linear trap has reduced the 2nd order Doppler shift by almost a factor of 10. This has been the largest source of potential frequency instabilities in previous lamp based Hg frequency standards. The degree of regulation required to reach 10^{-16} stability is also shown in the table.

The ion cloud temperature can be measured by propagating microwaves along the axis of the linear 12-pole as described in reference [21]. The 40.5 GHz transition will then be 1st order Doppler broadened to

$$\delta\nu = 2(\nu_0/c)\sqrt{\frac{2k_B T \ln 2}{m}} = 2.056\sqrt{T} \text{ kHz} = 35.6 \text{ kHz for } T=300 \text{ K. The width of this resonance could be}$$

measured to $\sim 5\%$ to determine the secular temperature 2nd Doppler offset to an uncertainty $\sim 10^{-14}$. The ion temperature stability may ultimately be determined by the ambient temperature variation since the buffer gas is at that temperature. The ambient 0.1 K temperature stability requirement for 10^{-16} clock operation is readily met in most frequency standard labs.

Frequency Offset	Magnitude	Projected Absolute Uncertainty	Regulation Required To reach 10^{-16}
Second-order Doppler			
Secular ($\sim 300\text{K}$)	2.4×10^{-13}	1×10^{-14}	Ion Temperature $\sim 0.1\text{K}$
Space-Charge induced micromotion	2×10^{-14}	$< 10^{-14}$	Ion Number $\sim 0.5\%$
Second-order Zeeman (@ 35 mG)	3×10^{-12}	1×10^{-14}	$\sim 5 \times 10^{-7}$ Gauss
Helium Buffer Gas	1.1×10^{-13}	10^{-14}	$\sim 10^{-8}$ mBar
AC Zeeman	$< 10^{-14}$	$< 10^{-14}$	$\sim 1\%$

SUMMARY

There has been considerable progress in the last two decades since trapped ion standards were first realized. Clocks based on mercury ions in linear traps are already operational, and support deep space navigation in the NASA Deep Space Complex. New developments based on multipole traps promise the realization of small,

highly stable clocks with enough accuracy to support space borne applications. Meanwhile, with advances in lasers and associated technologies, laser cooled ion clocks are also approaching the goal of evolving out of the laboratory, into field applications. These and other emerging improvements will make future trapped ion clocks and frequency standards available to a much larger class of applications, ranging from tests of fundamental physics, to navigation on Earth and on planetary surfaces.

ACKNOWLEDGMENTS

This work was carried out at the Jet Propulsion Laboratory, California Institute of Technology, under a contract with the National Aeronautics and Space Administration. The authors thank Dr. B. C. Young for useful comments regarding this manuscript.

REFERENCES

1. G. John Dick, Rabi T. Wang, and Robert L. Tjoelker, "Cryo-Cooled Sapphire Oscillator with Ultra-High Stability," *Proceedings of the 1998 IEEE International Frequency Control Symposium*, 1998, pp. 528-533.
2. D. J. Berkeland, J. D. Miller, J. C. Bergquist, W. M. Itano, and D. J. Wineland, *Phys. Rev. Lett.* **80**, 2089-2092 (1998).
3. R. F. Wuerker, H. Sheldon, and R. V. Langmuir, 'Electrodynamic Containment of Charged Particles,' *J. Appl. Phys.* **30**, 342-349 (1959).
4. H. G. Dehmelt, 'Radio-Frequency Spectroscopy of Stored Ions I: Storage,' *Advances in Atomic and Molecular Physics* **3**, 53-72 (1969).
5. P. T. H. Fisk, 'Trapped Ion and Trapped Atom Microwave Frequency Standards,' *Rep. Prog. Phys.* **60**, 761-818 (1997).
6. D. J. Berkeland, J. D. Miller, F. C. Cruz, B. C. Young, R. J. Rafac, X. -P. Huang, W. M. Itano, J. C. Bergquist and D. J. Wineland, 'High-Resolution, High-Accuracy Spectroscopy of Trapped Ions,' *Atomic Physics* **16**, 29-41, eds., W. E. Baylis and G. W. F. Drake, AIP CP477 (1999).
7. J. D. Prestage, R. L. Tjoelker, G. J. Dick, and L. Maleki, *J. Mod. Optics* **39**, 221-232 (1992).
8. J. J. Bollinger, D. J. Heinzen, W. M. Itano, S. L. Gilbert, and D. J. Wineland, 'A 303-MHz Frequency Standard Based on Trapped Be^+ Ions,' *IEEE Trans. Instrum. Meas.* **40**, 126 (1991).
9. U. Tanaka, H. Imajo, K. Hayasaka, R. Omukai, M. Watanabe, and S. Urabe, *Phys. Rev. A* **53**, 3982-3985 (1996).
10. G. J. Dick and C. A. Greenhall, *Proc. 1998 IEEE International Frequency Control Symposium*, 99-103 (1998)
11. P. Lemonde, G. Santarelli, Ph. Laurent, F. Pereira Dos Santos, A. Clairon and C. Salomon, *Proc. 1998 IEEE International Frequency Control Symposium*, 110-115 (1998).
12. J. Hoffnagle, R. G. Devoe, L. Reyna, and R. G. Brewer, *Phys. Rev. Lett.* **61**, 255 (1988); R. G. Brewer, J. Hoffnagle, R. G. Devoe, L. Reyna, and W. Henshaw, *Nature* (London) **344**, 305 (1990).
13. R. Blumel, J. M. Chen, E. Peik, W. Quint, W. Schleich, Y. R. Shen, and H. Walther, *Nature* (London) **334**, 309 (1988); R. Blumel, C. Kappler, W. Quint, and H. Walther, *Phys. Rev. A* **40**, 808 (1989).
14. J. D. Prestage, G. J. Dick, and L. Maleki, *J. Appl. Phys.* **66**, 1013-1017 (1989).
15. R. B. Warrington, P. T. H. Fisk, M. J. Wouters, M. A. Lawn, and C. Coles, 'The CSIRO Trapped $^{171}\text{Yb}^+$ Ion Clock: Improved Accuracy through Laser-Cooled Operation' in *Proc. 1999 Joint EFTF/IEEE International Frequency Control Symposium*, to be published.
16. J. D. Prestage, R. L. Tjoelker, G. J. Dick, and L. Maleki, *Proceedings of the 1993 IEEE International Frequency Control Symposium*, 144-147 (1993).
17. D. Gerlich, 'Inhomogeneous RF Fields: A Versatile Tool for the Study of Processes with Slow Ions,' *Adv. Chem. Phys.* **LXXXII**, 1-176 (1992).

18. L. S. Cutler, C. A. Flory, R. P. Giffard, and M. D. McGuire, *Appl. Phys. B* **39**, 251-259 (1986); L. S. Cutler, R. P. Giffard, and M. D. McGuire, 'A Trapped Mercury 199 Ion Frequency Standard,' *Proc. 13th Ann. PTI Application and Planning Meeting*, NASA Conf. Pub. 2220, 563-578 (1981).
19. J. D. Prestage, R. L. Tjoelker, and L. Maleki, 'Higher Pole Linear Traps for Atomic Clock Applications', in *Proc. 1999 Joint EFTF/IEEE International Frequency Control Symposium*, to be published.
20. G. R. Janik, J. D. Prestage, and L. Maleki, *J. Appl. Phys.* **67**, 6050-6055 (1990).
21. J. D. Prestage, R. L. Tjoelker, G. J. Dick, and L. Maleki, *Proc. 1993 IEEE International Frequency Control Symposium*, 148-154, Salt Lake City, USA (1993).